

Mn-substituted perovskites $\text{RECo}_x\text{Mn}_{1-x}\text{O}_3$: a comparison between magnetic properties of $\text{LaCo}_x\text{Mn}_{1-x}\text{O}_3$ and $\text{GdCo}_x\text{Mn}_{1-x}\text{O}_3$

C. CAMPOS¹, G. PECCHI¹, Y. MORENO¹, C. MOURE², V. GIL², P. BARAHONA³, O. PEÑA⁴

¹ Facultad de Ciencias Químicas, Universidad de Concepción, Concepción, Chile

² Instituto de Cerámica y Vidrio, CSIC, Electroceramics Department, 28049 Madrid, Spain

³ Instituto de Ciencias Básicas, Universidad Católica del Maule, Talca, Chile

⁴ Sciences Chimiques de Rennes, UMR 6226, Université de Rennes 1, 35042 Rennes, France

Cooperative phenomena constitute important mechanisms to explain the magnetic properties of the perovskite manganites REMnO_3 , in which the rare-earth and/or Mn is partially replaced by divalent elements. In this way, the manganese ion changes its valence state ($\text{Mn}^{3+} \rightarrow \text{Mn}^{4+}$), triggering strong magnetic interactions. In this work we describe the case of $\text{GdCo}_x\text{Mn}_{1-x}\text{O}_3$ ($0.0 \leq x \leq 1.0$) for which the antiferromagnetic interaction between the Gd sublattice and the Mn/Co network leads to a reversal of the magnetic moment at low temperature. No inversion is observed for the $\text{LaCo}_x\text{Mn}_{1-x}\text{O}_3$ series, in which the ordering temperature may attain a maximum of 235 K for $\text{LaCo}_{0.50}\text{Mn}_{0.50}\text{O}_3$, while it is only 120 K for similar Co/Mn ratio in the case of $\text{GdCo}_{0.50}\text{Mn}_{0.50}\text{O}_3$.

Magnetic properties are described in terms of two regimes: one, for $x < 0.5$, when Co substitutes Mn in the GdMnO_3 manganite and another one, for $x > 0.5$, when Mn substitutes Co in the GdCoO_3 cobaltite, while the magnetic interactions are maximized at $x(\text{Co}) = 0.50$. This hypothesis is discussed in terms of the respective oxidation states of both manganese ($\text{Mn}^{3+} / \text{Mn}^{4+}$) and cobalt ($\text{Co}^{2+} / \text{Co}^{3+}$).

Keywords: Perovskites, Magnetic Oxides, Ferromagnetic Properties, Mixed Valence.

Perovskitas manganitas con Mn sustituido $\text{TRCo}_x\text{Mn}_{1-x}\text{O}_3$: comparación entre las propiedades magnéticas de $\text{LaCo}_x\text{Mn}_{1-x}\text{O}_3$ y de $\text{GdCo}_x\text{Mn}_{1-x}\text{O}_3$

El fenómeno cooperativo constituye un importante mecanismo para explicar las propiedades magnéticas de las perovskitas manganitas TRMnO_3 , en las que el catión de tierra rara, TR, y/o el catión Mn^{3+} son parcialmente reemplazados por cationes divalentes. Por esta vía el ión de manganeso cambia de estado de valencia ($\text{Mn}^{3+} \rightarrow \text{Mn}^{4+}$), generando fuertes interacciones magnéticas. En el presente trabajo se describe el caso de las soluciones sólidas $\text{GdCo}_x\text{Mn}_{1-x}\text{O}_3$ ($0.0 \leq x \leq 1.0$) para las que la interacción antiferromagnética entre la subred del Gd^{3+} y la red Mn/Co lleva a una inversión del momento magnético a baja temperatura. No se ha observado inversión para la serie $\text{LaCo}_x\text{Mn}_{1-x}\text{O}_3$, en que la temperatura de orden puede alcanzar un máximo de 235K para $\text{LaCo}_{0.50}\text{Mn}_{0.50}\text{O}_3$, mientras que en el caso de $\text{GdCo}_{0.50}\text{Mn}_{0.50}\text{O}_3$, en que sí se observa inversión, la temperatura de orden es sólo de 120 K para una razón Co/Mn similar.

Las propiedades magnéticas se describen en términos de dos regímenes diferentes: uno, para $x < 0.5$, cuando Co sustituye al Mn en la manganita GdMnO_3 y otro, para $x > 0.5$, cuando Mn sustituye a Co en la cobaltita GdCoO_3 . Las interacciones magnéticas se maximizan a $x(\text{Co}) = 0.50$. Esta hipótesis se discute en términos de los respectivos estados de oxidación de ambos cationes: manganeso ($\text{Mn}^{3+} / \text{Mn}^{4+}$) y cobalto ($\text{Co}^{2+} / \text{Co}^{3+}$).

Palabras clave: Perovskitas, Óxidos Magnéticos, Propiedades Ferromagnéticas, Valencias mixtas

1. INTRODUCTION

Mixed-valence perovskites ABO_3 have been thoroughly studied in the last 20 years because of their exceptional magneto-electrical properties (1). Most of these reports concern the substitution of the rare-earth located at the A site by alkaline-earth AE elements $\text{RE}_{1-x}\text{AE}_x\text{MnO}_3$ since, by this way, the Mn^{3+} cation transforms into $x\text{-Mn}^{4+}$ ions, triggering the well-known double-exchange ferromagnetic interactions (2). Substitution of Mn located at the B-site by a divalent transition metal Me element $\text{REMe}_x\text{Mn}_{1-x}\text{O}_3$ is also a good way to transform $2x\text{-Mn}^{3+}$ into $x\text{-Mn}^{4+}$ ions (one manganese being replaced, the other one, transforming). Substitutions at the B-site have been rarely studied in the past, in comparison with

the classical A-site substitution. Some works have reported the $\text{Mn} \rightarrow \text{Co}$ or $\text{Mn} \rightarrow \text{Ni}$ cases (3-5) while systematic substitutions have been reported by our research groups in the yttrium-based perovskite $\text{YMe}_x\text{Mn}_{1-x}\text{O}_3$ (6-8). Recently, we have extended our studies to perovskite systems $\text{REMe}_x\text{Mn}_{1-x}\text{O}_3$, in which the lanthanide ion is a heavy rare-earth of small ionic radius and large magnetic moment (e.g., RE = Gd, Er) (9,10). One of the particularities of these latter compounds is the relative small ordering temperature T_c , much lower than those found for large rare-earth elements since, the smaller the RE ionic radii, the more distorted is the perovskite structure and the largest is the deviation of the $\text{Mn}^{3+}\text{-O-Mn}^{4+}$ chain from an

ideal 180°-angle, this latter being related to the highest T_c 's (11).

Our present goal is to synthesize $\text{REMe}_x\text{Mn}_{1-x}\text{O}_3$ systems with big lanthanide cations, (i.e., high ordering temperatures) and to compare the different interaction mechanisms with those observed in similar compounds with small cations. Our choice was aimed this time toward $\text{RE} = \text{La}$ and Gd , $\text{Me} = \text{Co}$, since the full range of the solid solutions ($0 \leq x \leq 1$) is available, provided strict synthesis routes are respected. We present herein the magnetic properties of $\text{LaCo}_x\text{Mn}_{1-x}\text{O}_3$, prepared by soft chemistry techniques (i.e., very fine particles synthesized at mild temperatures, appropriate for catalysis (12) making a comparison with gadolinium-based $\text{GdCo}_x\text{Mn}_{1-x}\text{O}_3$ prepared by high-temperature solid-state methods (9).

2. EXPERIMENTAL PROCEDURE

$\text{LaCo}_x\text{Mn}_{1-x}\text{O}_3$ perovskites were prepared by the citrate method. Stoichiometric amounts of an aqueous solution of the nitrates of the corresponding metals were added to an aqueous solution of citric acid with a 10 % excess over the number of ionic equivalents of cations. The resulting solution was stirred at room temperature and slowly evaporated at 70 °C under vacuum in a rotary evaporator until gel is formed. This gel was dried in an oven, slowly increasing the temperature up to 250 °C and maintained overnight to yield a solid amorphous citrate precursor. The resulting powder was crushed, sieved and calcined at 700 °C in air for 6 h. Our requirements to use this powder for catalysis purposes made us work under such mild conditions, thus obtaining BET surfaces of the order of 10-40 $\text{m}^2\cdot\text{g}^{-1}$ (12). The average crystallites size, as calculated from XRD data using the classical Scherrer's relation, ranged between 26 and 50 nm.

$\text{GdCo}_x\text{Mn}_{1-x}\text{O}_3$ perovskites were prepared by solid state reaction of reagent grade MnO , CoO and Gd_2O_3 oxides of submicronic particle size. The mixtures were homogenized by attrition milling, using isopropanol as liquid medium. The dried mixtures were calcined at 1150 °C for 2h, then re-milled and dried, granulated, and uniaxially pressed. Sintering was performed under oxygen atmosphere for 2 hours, at temperatures ranging between 1250 °C and 1350 °C, i.e. below those needed to get a maximum of the apparent density. In this way, compact specimens devoted to technological applications (magnetoresistance, electroceramic devices, etc.) could be prepared. The remaining porosity favours a proper oxygenation at the grains surface, as confirmed by the weight gain after sintering. The choice of the sintering conditions took also into account the fact that cobalt may be volatile at high temperatures, the lower sintering temperature corresponding then to samples with higher amount of Co (10,13). EDX analysis confirmed the nominal Co/Mn ratio, within 5 % error. The cooling rate was 1 °C/min, still under oxygen flow, thus favouring the insertion of the maximum quantity of oxygen in the structure (13).

At this point we should insist on the fact that, even both series were synthesized and annealed under different conditions, optimum oxygenation could be accomplished in both cases (at mild temperatures, under air, for tiny particles of large specific area, or at high temperatures followed by slow cooling under oxygen, for compact specimens). Magnetic data discussed below will confirm these assertions since the expected transformations of the Mn oxidation state were achieved in similar manner in both series.

X-ray powder diffraction (XRD) patterns were obtained with Ni-filtered $\text{CuK}\alpha_1$ radiation ($\lambda = 1.5418 \text{ \AA}$) using a Rigaku (La-based perovskites) or a D-5000 Siemens diffractometer (Gd-based perovskites), at a scanning rate of $2^\circ 2\theta/\text{min}$. Crystallochemical properties are given elsewhere (9,12). Magnetic measurements were performed in a Quantum Design MPMS-XL5 SQUID susceptometer, between 2 K and 300 K and as a function of the applied field, from -50 kOe up to +50 kOe. All measurements were done in specimens (ceramics or compacted powder) glued to sample holders, thus avoiding any disorientation due to torque forces exerted on the sample.

3. RESULTS

3.1. Paramagnetic regime

Figure 1 shows the inverse susceptibility for the series $\text{LaCo}_x\text{Mn}_{1-x}\text{O}_3$. Two regimes are clearly identified: for cobalt contents between 0 and 0.50, the Curie-Weiss temperature Θ keeps increasing, with a smooth variation of the slope $|\Delta\chi^{-1}/\Delta T|$ (strangely, these curves converge toward the same value at 400 K, but this must be considered as fortuitous and no physical argument should be evoked). Samples with $x(\text{Co}) > 0.5$ showed, on the other hand, a progressive decrease of Θ , reaching a largely negative value of -195 K for the undoped cobaltite LaCoO_3 . This tendency is hardly observed in $\text{GdCo}_x\text{Mn}_{1-x}\text{O}_3$ because the strong magnetic moment of Gd hinders that of the Mn/Co network. The characteristic temperatures follow similar variations in both systems, as shown in figure 2, where the Curie-Weiss Θ and the ordering T_c temperatures are plotted as a function of the cobalt content. The ferromagnetic interactions are maximized at the substitution rate $\text{Co}:\text{Mn}=0.5:0.5$, for which the charge equilibrium relation should be $\text{RE}^{3+}\text{Co}_{0.5}^{2+}\text{Mn}_{0.5}^{4+}\text{O}_{2-3}^{2-}$ (14). However, obvious differences are observed in the overall variation of Θ : while in the case of lanthanum-based perovskites, it remains positive and relative high (except for the end compound, LaCoO_3), in the case of gadolinium-based perovskites there is a net tendency to become negative at both ends of the solid solution. This is a clear demonstration that antiferromagnetic

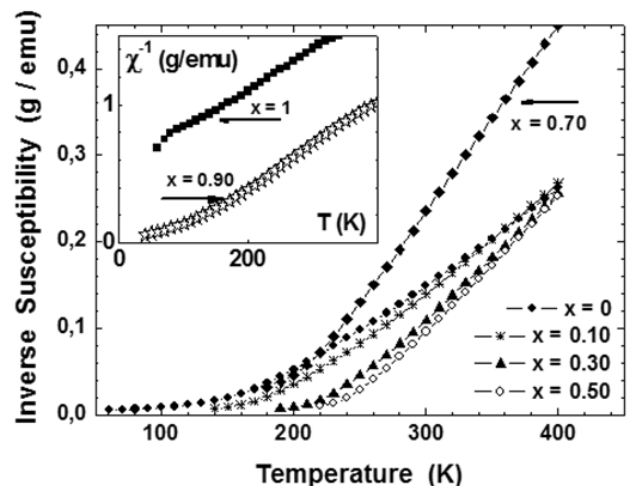


Fig. 1- Inverse magnetic susceptibility for the solid solution $\text{LaCo}_x\text{Mn}_{1-x}\text{O}_3$. Inversa de la susceptibilidad magnética para la solución sólida $\text{LaCo}_x\text{Mn}_{1-x}\text{O}_3$.

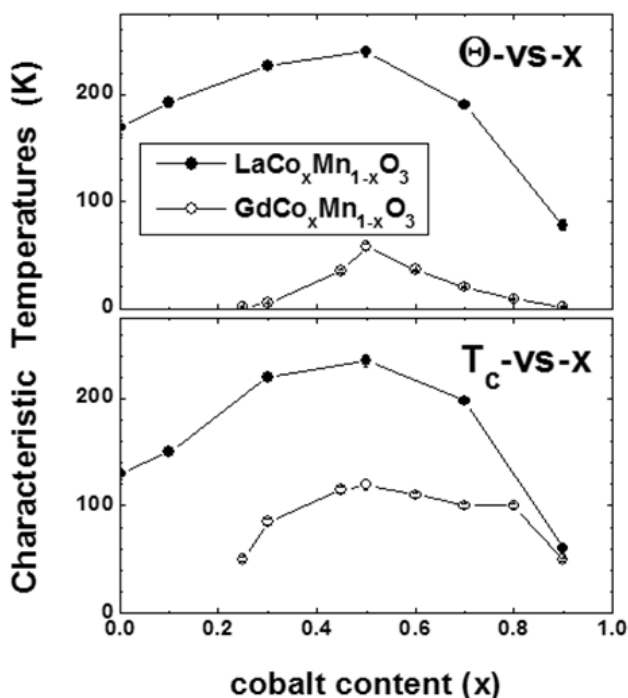


Fig. 2- Characteristic temperatures Θ (upper panel) and T_c (lower panel) for solid solutions $\text{LaCo}_x\text{Mn}_{1-x}\text{O}_3$ (filled symbols) and $\text{GdCo}_x\text{Mn}_{1-x}\text{O}_3$ (open symbols). Temperaturas Características Θ (recuadro superior) y T_c (recuadro inferior) para las soluciones sólidas $\text{LaCo}_x\text{Mn}_{1-x}\text{O}_3$ (símbolos llenos) y $\text{GdCo}_x\text{Mn}_{1-x}\text{O}_3$ (símbolos vacíos).

interactions must be considered, this behavior being more pronounced in $\text{GdCo}_x\text{Mn}_{1-x}\text{O}_3$ than in $\text{LaCo}_x\text{Mn}_{1-x}\text{O}_3$.

This marked difference is also observed in the effective moments of the paramagnetic state. For $\text{LaCo}_x\text{Mn}_{1-x}\text{O}_3$ (12), the effective moments for the first half of the series ($x \leq 0.50$) are systematically higher than the moments expected for corresponding mixtures of Mn^{3+} , Mn^{4+} and Co^{2+} ions, while for the second half, they are systematically lower than expected. We explain these results by the fact that strong Co^{2+} - Mn^{4+} double-exchange interactions via the oxygen (15) are triggered when Co^{2+} is introduced into the lattice ($x \leq 0.50$), while antiferromagnetism is advantaged when cobalt is introduced as Co^{3+} ($x > 0.50$). For $\text{GdCo}_x\text{Mn}_{1-x}\text{O}_3$ (9), the effective moments of the transition metals (after subtraction of the Gd contribution) are always lower than the expected values for any combination of Mn and Co ionic moments, meaning that antiferromagnetic interactions must be considered all over the solid solution.

The characteristic temperatures Θ and T_c observed in $\text{La}(\text{Co},\text{Mn})\text{O}_3$ are quite high (+240 K and 235 K, respectively), while in $\text{Gd}(\text{Co},\text{Mn})\text{O}_3$ they amount to only +58 K and 120 K, for the respective $\text{RECo}_{0.50}\text{Mn}_{0.50}\text{O}_3$ compositions. This fact is not new since it is well known that the largest the ionic radii, the highest are the ordering temperatures (11).

3.2. Ordered regime

3.2.1. ZFC/FC cycles

The ordered regime was investigated through magnetization ZFC/FC cycles as a function of temperature. Because of the very low applied field (250 Oe or lower), the

rare-earth contribution is, in first approximation, neglected and only the ordered network should be observed during the warm-up (ZFC). As a consequence, the warming branches must be similar for both families of compounds, since they reflect essentially the magnetic behavior of the transition metal |Co+Mn| network, that is, a canted-type magnetic structure where antiferromagnetic inter-plane exchange competes with ferromagnetic intra-plane interactions (16-18). The predominant antiferromagnetic component appears as a pronounced peak during warming, as seen in figures 3.a and 3.b (open symbols) for $\text{LaCo}_x\text{Mn}_{1-x}\text{O}_3$ and $\text{GdCo}_x\text{Mn}_{1-x}\text{O}_3$. In the case of the gadolinium-based system, a faint Curie-Weiss variation appears at low temperature, whereas no additional contribution is observed for non-magnetic lanthanum.

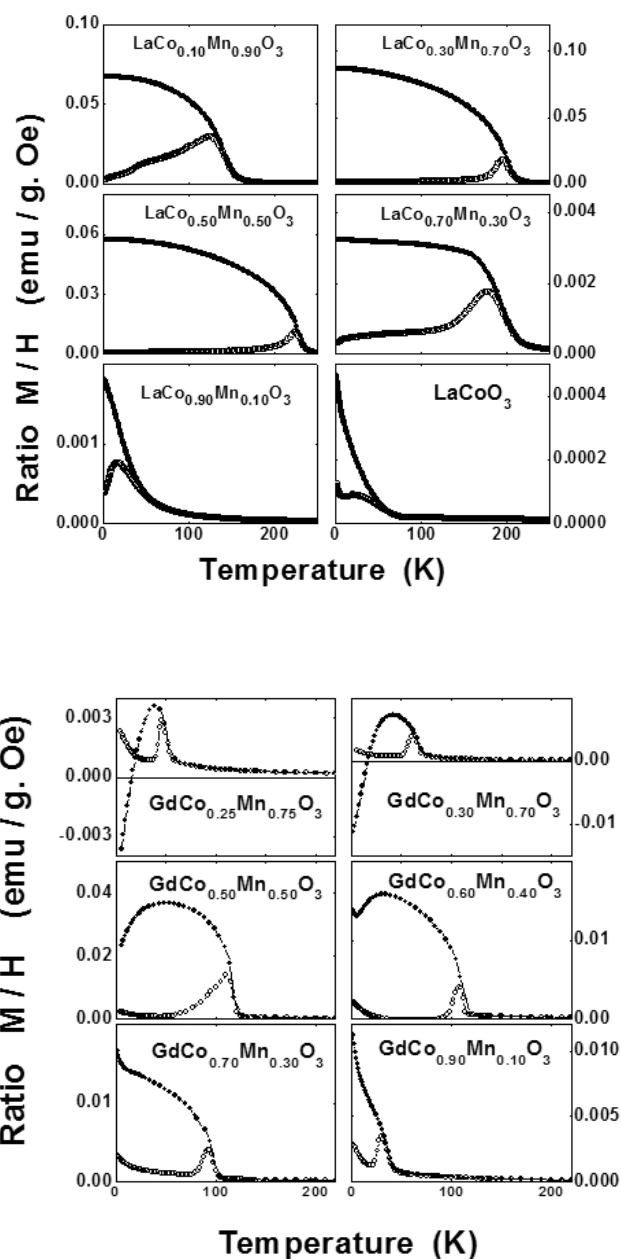


Fig. 3- Magnetization ZFC/FC cycles for : (a) $\text{LaCo}_x\text{Mn}_{1-x}\text{O}_3$, (b) $\text{GdCo}_x\text{Mn}_{1-x}\text{O}_3$. Ciclos de magnetización ZFC/FC para: (a) $\text{LaCo}_x\text{Mn}_{1-x}\text{O}_3$, (b) $\text{GdCo}_x\text{Mn}_{1-x}\text{O}_3$.

Contrary to this, the field-cooled FC procedure (closed symbols in figs. 3.a and 3.b) is dramatically different for both series, since the transition-metal network orders at T_c and imposes a strong internal field over the rare-earth spins. The local field attains 5 kOe or more, that is, a factor 20 \times with respect to the applied external field (19) and, as a consequence, the rare-earth magnetization may become predominant over the contribution of the transition-metal moment. The resulting magnetization will be the superposition of the relative magnetizations, one due to the transition metals $|Co+Mn|$, and the other one due to the rare-earth network. It is expected then, for non-magnetic lanthanum, that the only contribution in the $LaCo_xMn_{1-x}O_3$ series must be the ferromagnetic behavior of the transition metal network (schematized by a step-like transition with $M = 0$ at $T > T_c$; $M = M_{|Co+Mn|}$ at $T < T_c$). As shown in figure 3.a, the ferromagnetic interactions are optimized when inserting cobalt in the first half of the series since T_c progressively increases; this strong ferromagnetic behavior is also visible through the characteristic plateau of the magnetization M_{FC} during cooling. At the other end, for $LaCo_{0.90}Mn_{0.10}O_3$ and $LaCoO_3$, the magnetization M_{FC} keeps increasing when cooling the sample although it attains very low values at 2 K (notice the enormous difference in the Y-scales in fig. 3.a with respect with the first half of the series).

The situation is radically different in $GdCo_xMn_{1-x}O_3$ (fig. 3.b) since a large magnetic contribution is expected because of the strong moment of gadolinium ($4f^7$; $\mu_{eff} = 7.94 \mu_B$). By considering these latter as independent, uncoupled Gd ions, with no 4f-4f interactions, a Curie-Weiss-like magnetization should exist, superposed to the step-like magnetization of the transition metal network. Under the hypothesis of a negative exchange interaction between magnetic sublattices, that is, magnetic moments oriented in opposite directions, a ferrimagnetic-like situation may occur, in which the total moment ($M_{tot} = M_{Gd} + M_{|Co+Mn|}$) will reverse its sign during cooling when M_{Gd} exceeds the value of $M_{|Co+Mn|}$. Such situation occurs because the Curie-Weiss susceptibility for non-correlated Gd spins varies as T^{-1} , increasing when the temperature decreases, while the magnetization of the transition metal stays constant below T_c . A full description of this process in terms of a mean-field model of interacting sublattices can be found in ref. (19,20) for $(Gd,Ca)MnO_3$ or ref. (9) for $Gd(Me,Mn)O_3$ ($Me = Cu, Ni, Co$).

The nature of the exchange interaction between gadolinium and transition-metal sublattices changes along the $GdCo_xMn_{1-x}O_3$ series. At low cobalt concentrations (fig. 3.b, upper panels) the ferromagnetic order is mainly due to the $Mn^{3+}-Mn^{4+}$ pairs, since a similar situation is observed in $Gd_{1-x}Ca_xMnO_3$ where no cobalt atom exists (19). When increasing $x(Co)$, Mn^{3+} is progressively substituted by Co^{2+} , which is also ferromagnetically coupled to Mn^{4+} since the ferromagnetic ordering temperature T_c increases steadily. The ferromagnetic interactions $Co^{2+}-Mn^{4+}$ are optimized at $x(Co) = 0.50$ when all Mn^{3+} have been replaced by Co^{2+} (fig. 3.b, middle panels). At further substitutions, the quantity of Mn atoms decreases, resulting in fewer numbers of Co^{2+}/Mn^{4+} pairs; from charge equilibrium arguments (13), the cobalt being now introduced into the lattice is trivalent and the resulting $Co^{3+}-Mn^{4+}$ interactions are of different nature as the $Co^{2+}-Mn^{4+}$ interactions. The ordering temperature decreases and the gadolinium network is not any longer polarized negatively with respect to the transition-metal network (fig. 3.b, bottom panels).

3.2.2. Magnetization M(H) cycles

The ordered regime was also investigated through magnetization loops at 2 K. In the case of $LaCo_xMn_{1-x}O_3$ (fig. 4.a), two distinct regimes are observed: when $x(Co)$ goes from 0 to 0.5, a systematic increase of the coercive field H_{coerc} is observed, while the "saturation" magnetization M_{sat} (value at 50 kOe) stays almost unchanged; when $x(Co)$ exceeds 0.5, both H_{coerc} and M_{sat} decrease rapidly, reaching almost zero for lanthanum cobaltite (insert, fig. 4.a). Qualitatively these different behaviors can be described, during the first regime, by an ideal squared-shape ferromagnetic loop, with a linear increase of H_{coerc} (rate ~ 26 kOe/at.Co) related to an increasing number of domains proportional to the number of pairs Co^{2+}/Mn^{4+} . In the second regime, for $x > 0.5$, $M(H)$ is a superposition of ferromagnetism and antiferromagnetism since the presence of Co^{3+} triggers antiferromagnetic interactions with Mn^{4+} and/or Co^{2+} .

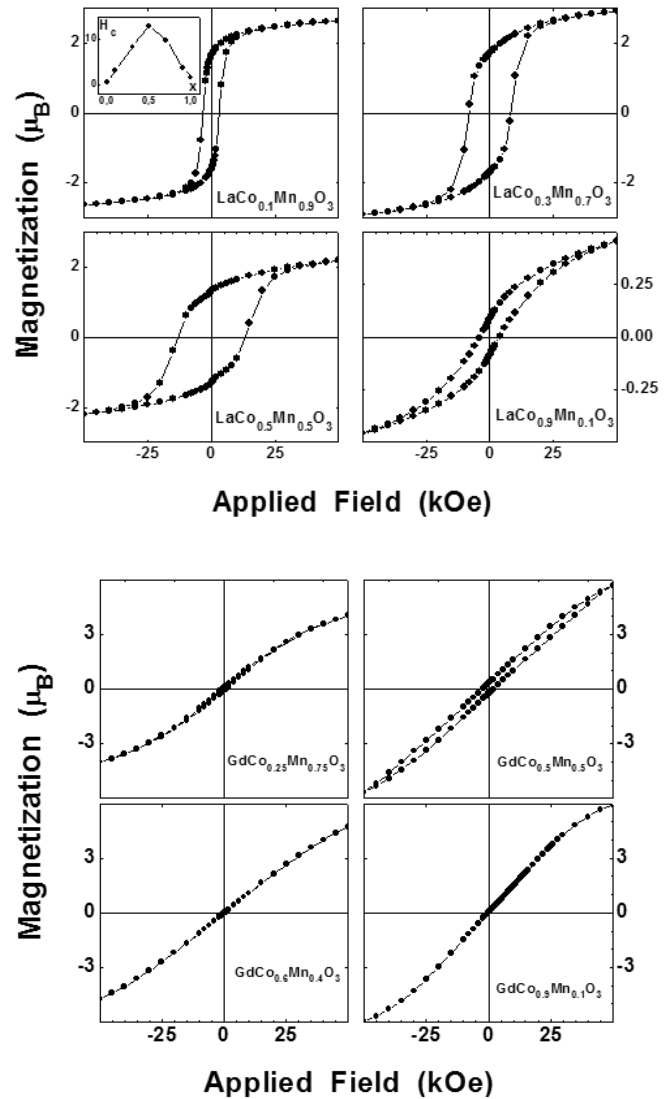


Fig. 4- Magnetization loops at $T = 2$ K for : (a) $LaCo_xMn_{1-x}O_3$ (b) $GdCo_xMn_{1-x}O_3$ (insert in fig. 4.a shows the compositional variation of the coercive field, in units of kOe). Curvas de magnetización a $T = 2$ K para: (a) $LaCo_xMn_{1-x}O_3$, (b) $GdCo_xMn_{1-x}O_3$ (recuadro en fig. 4.a muestra la variación composicional del campo coercitivo, en unidades de kOe).

The magnetization loops for $\text{GdCo}_x\text{Mn}_{1-x}\text{O}_3$ (figure 4.b) differ significantly from the previous ones. Because of the antiferromagnetic exchange between the Gd and the transition metals networks, the antiferromagnetic component dominates in all samples. The coercive field H_{coerc} is very low at low cobalt-substitution, reaching a maximum at $x(\text{Co}) = 0.50$ (approximately 2 kOe, compared to 13 kOe for similar composition of $\text{LaCo}_x\text{Mn}_{1-x}\text{O}_3$).

4. DISCUSSION

It becomes evident from the above results, that the solid solutions $\text{RECO}_x\text{Mn}_{1-x}\text{O}_3$ can be analyzed through two different approaches: either, as substituting cobalt in the rare-earth manganite REMnO_3 , or as substituting manganese in the rare-earth cobaltite RECoO_3 . In the first case, the Mn^{3+} - Mn^{4+} and Co^{2+} - Mn^{4+} ferromagnetic interactions predominate, leading toward an optimization of the ferromagnetic state when all manganese is converted into Mn^{4+} (i.e., when $\text{RE}^{3+}\text{Co}^{2+}_{0.5}\text{Mn}^{4+}_{0.5}\text{O}_3$). In the second case, two different approaches can be considered: either Mn enters the solid solution as a trivalent cation, so the charge equilibrium is unchanged with cobalt as Co^{3+} , or Mn enters as tetravalent ion, transforming an additional cobalt ion into Co^{2+} . All our results point towards this second possibility, since strong Co^{2+} - Mn^{4+} ferromagnetic interactions are observed according to a charge equilibrium $\text{RE}^{3+}\text{Co}^{2+}_x\text{Mn}^{3+}_{1-2x}\text{Mn}^{4+}_x\text{O}_3$.

From these considerations it is quite obvious that transformations $\text{Mn}^{3+} \rightarrow \text{Mn}^{4+}$ and presence of Co^{2+} and Co^{3+} operate similarly in both solid solutions, independent of the technique of synthesis, thus reinforcing our hypothesis of optima oxygenation conditions (§2, Experimental section). The reported differences in magnetic behavior come, in fact, from the different magnetic nature between La ($4f^0$) and Gd ($4f^7$) elements, the first one being nonmagnetic, and the latter one interacting antiferromagnetically with the transition metal network.

A final remark concerns LaCoO_3 and GdCoO_3 since a large amount of reports refer to the cobaltite end-members $x(\text{Co}) = 1$. These pure cobaltites have been thoroughly studied because of the magnetic-electronic transitions observed at low and high temperatures and the different anomalies associated to them (21,22). It is by now established that a spin transition occurs from a low-temperature low-spin LS state $\text{Co}^{\text{III}} (t^6_e^0; S = 0)$ toward a high-temperature high-spin HS state $\text{Co}^{3+} (t^4_{2g}e^2_g; S = 2)$, although an intermediate spin IS state $(t^5_{2g}e^1_g; S = 1)$ has been also suggested (22). The magnetic properties of these parent compounds are extremely dependent on hole-doping at the RE^{3+} site; in this way, spin transitions may locally occur on a Co site and provoke double-exchange mechanisms responsible of the slight ferromagnetic components. It has been shown, for instance, that doping levels of about two holes per thousand Co^{3+} may transform a diamagnetic insulator state into a paramagnetic compound (23).

4. CONCLUSIONS

The mixed-valence states of manganese and cobalt ions have been characterized in two perovskite systems $\text{RE}(\text{Co,Mn})\text{O}_3$. For $\text{RE} = \text{La}$, which has no intrinsic moment, the magnetic behavior of the Co/Mn lattice is observed. For $\text{RE} = \text{Gd}$, the Gd and the transition metal (Co+Mn) sublattices interact

antiferromagnetically, leading to a ferrimagnetic state and eventually, to a reversal of the total magnetic moment.

The particular substitution rate $\text{Co:Mn}=0.5:0.5$ represents a frontier composition, for which the ferromagnetic interactions are maximized (largest coercive field, highest ordering temperature, largest magnetization values, etc.). In the region $0 < x(\text{Co}) \leq 0.50$, these systems can be described as if the Co cation substitutes Mn in the REMnO_3 manganite, enhancing the ferromagnetic interactions because of the presence of Mn^{3+} - Mn^{4+} and Co^{2+} - Mn^{4+} pairs. In the region $0.5 < x(\text{Co}) < 1$, they can be described as if tetravalent Mn^{4+} substitutes Co^{3+} in the RECoO_3 cobaltite, with weak ferromagnetic interactions within an overall antiferromagnetic system.

ACKNOWLEDGMENTS

Authors acknowledge the bilateral exchange programs France-Spain CNRS-CSIC, project n° 18873 and France-Chile ECOS-CONICYT, project C05E01. National projects from Chilean government, FONDECYT 1060702 and FONDECYT 11060462, are also acknowledged for financial support.

REFERENCES

1. Y. Tokura, Colossal magnetoresistive oxides, Gordon & Breach, New York, 2000
2. E.O. Wollan, W.C. Koehler, Neutron diffraction study of the magnetic properties of the series of perovskite-type compounds $[(1-x)\text{La}, x\text{Ca}]\text{MnO}_3$, Phys. Rev., 100(2) 545-563 (1955)
3. N. Gayathri, A.K. Raychaudhuri, S.K. Tiwary, R. Gundakaram, A. Arulraj, C.N.R. Rao, Electrical transport, magnetism, and magnetoresistance in ferromagnetic oxides with mixed exchange interactions: A study of the $\text{La}_{0.7}\text{Ca}_{0.3}\text{Mn}_{1-x}\text{Co}_x\text{O}_3$, Phys. Rev. B, 56(3), 1345-1353 (1997)
4. Z. Yang, L. Ye, X. Xie, Electronic and magnetic properties of the perovskite oxides: $\text{LaMn}_{1-x}\text{Co}_x\text{O}_3$, Phys. Rev. B, 59(10), 7051-7057 (1999)
5. K. Ghosh, S.B. Ogale, R. Ramesh, R.L. Greene, T. Venkatesan, K.M. Gapchup, R. Bathe, S.I. Patil, Transition-element doping effects in $\text{La}_{0.7}\text{Ca}_{0.3}\text{MnO}_3$, Phys. Rev. B, 59(1), 533-537 (1999)
6. O. Peña, M. Bahout, D. Gutiérrez, J.F. Fernández, P. Durán, C. Moure, Critical behavior in the perovskite-like system $\text{Y}(\text{Ni,Mn})\text{O}_3$, J. Phys. Chem. Solids, 61, 2019-2024 (2000)
7. D. Gutiérrez, O. Peña, K. Ghanimi, P. Durán, C. Moure, Electrical and magnetic features in the perovskite-type system $\text{Y}(\text{Co,Mn})\text{O}_3$, J. Phys. Chem. Solids, 63, 1975-1982 (2002)
8. D. Gutiérrez, O. Peña, P. Durán, C. Moure, Crystalline structure and electrical properties of $\text{YCu}_x\text{Mn}_{1-x}\text{O}_3$ solid solutions, J. Eur. Ceram. Soc., 22, 2939-2944 (2002)
9. O. Peña, A.B. Antunes, G. Martínez, V. Gil, C. Moure, Inter-network magnetic interactions in $\text{GdMeMn}_x\text{O}_3$ perovskites (Me = transition metal), J. Magn. Magn. Mater., 310, 159-168 (2007)
10. O. Peña, A.B. Antunes, M.N. Baibich, P.N. Lisboa-Filho, V. Gil, C. Moure, Spin reversal and magnetization jumps in $\text{ErMe}_x\text{Mn}_{1-x}\text{O}_3$ perovskites (Me = Ni, Co), J. Magn. Magn. Mater., 312, 78-90 (2007)
11. J.B. Goodenough, Localized-itinerant electronic transitions in oxides and sulfides, J. Alloys Compounds, 262-263, 1-9 (1997)
12. G. Pecchi, C. Campos, O. Peña, L.E. Cadus, Structural, magnetic and catalytic properties of perovskite-type mixed oxides $\text{LaMn}_y\text{Co}_3\text{O}_3$ ($y = 0.0, 0.1, 0.3, 0.5, 0.7, 0.9, 1.0$), J. Molec. Catalysis A: Chemical, 282, 158-166 (2008)
13. C. Moure, D. Gutiérrez, O. Peña, P. Durán, Effect of the processing parameters on the crystalline features of the solid solution $\text{Y}(\text{Co}_x\text{Mn}_{1-x})\text{O}_3$, $x=0.6, 0.7$, J. Am. Ceram. Soc., 86, 54-58 (2003)
14. C. Moure, D. Gutiérrez, O. Peña, P. Durán, Structural characterization of $\text{YMe}_x\text{Mn}_{1-x}\text{O}_3$ (Me = Cu, Ni, Co) perovskites, J. Solid. State Chem., 163, 377-384 (2002)
15. G. Blasse, Ferromagnetic interactions in non-metallic perovskites, J. Phys. Chem. Solids, 26(12), 1969-1971 (1965)
16. M. Hennion, F. Moussa, J. Rodríguez-Carvajal, L. Pinsard, A. Revcolevschi, Coherent waves of magnetic polarons propagating in $\text{La}_{1-x}\text{Ca}_x\text{MnO}_3$: An inelastic-neutron-scattering study, Phys. Rev. B, 56(2), R497-R500 (1997)
17. B. Dabrowski, X. Xiong, Z. Bukowski, R. Dybziński, P.W. Klamut, J.E. Siewenie, O. Chmaissem, J. Shaffer, C.W. Kimball, J.D. Jorgensen, S. Short,

- Structure-properties phase diagram for $\text{La}_{1-x}\text{Sr}_x\text{MnO}_3$ ($0.1 \leq x \leq 0.2$), *Phys. Rev. B*, 60(10), (1999) 7006-7017
18. J.M. De Teresa, C. Ritter, M.R. Ibarra, P.A. Algarabel, J.L. Garcia-Muñoz, J. Blasco, J. Garcia, C. Marquina, Charge localization, magnetic order, structural behavior, and spin dynamics of $(\text{La-Tb})_{2/3}\text{Ca}_{1/3}\text{MnO}_3$ manganese perovskites probed by neutron diffraction and muon spin relaxation, *Phys. Rev. B*, 56(6), 3317-3324 (1997)
 19. O. Peña, M. Bahout, K. Ghanimi, P. Durán, D. Gutiérrez, C. Moure, Spin reversal and ferrimagnetism in $(\text{Gd,Ca})\text{MnO}_3$, *J. Mater. Chem.*, 12, 2480-2485 (2002)
 20. G.J. Snyder, C.H. Booth, F. Bridges, R. Hiskes, S. DiCarolis, M.R. Beasley, T.H. Geballe, Local structure, transport, and rare-earth magnetism in the ferrimagnetic perovskite $\text{Gd}_{0.67}\text{Ca}_{0.33}\text{MnO}_3$, *Phys. Rev. B*, 55(10), 6453-6459 (1997)
 21. K. Asai, A. Yoneda, O. Yokokura, J.M. Tranquada, G. Shirane, K. Kohn, Two spin-state transitions in LaCoO_3 , *J. Phys. Soc. Japan*, 67(1), 290-296 (1998), and references therein
 22. K. Knížek, Z. Jiráček, J. Hejtmánek, M. Veverka, M. Maryško, G. Maris, T.T.M. Palstra, Structural anomalies associated with the electronic and spin transitions in LnCoO_3 , *Eur. Phys. J. B*, 47, 213-220 (2005)
 23. A. Podlesnyak, K. Conder, E. Pomjakushina, A. Mirmelstein, P. Allenspach, D.I. Khomskii, Effect of light Sr doping on the spin-state transition in LaCoO_3 , *J. Magn. Magn. Mater.*, 310, 1552-1554 (2007)

Recibido: 31.07.07

Aceptado: 20.12.07

